Bull. Mater. Sci., Vol. 38, No. 6, October 2015, pp. 1633–1638. © Indian Academy of Sciences.

Heating ability and biocompatibility study of silica-coated magnetic nanoparticles as heating mediators for magnetic hyperthermia and magnetically triggered drug delivery systems

MEYSAM SOLEYMANI and MOHAMMAD EDRISSI*
Department of Chemical Engineering, Amirkabir University of Technology, Hafez Ave., 15875-4413 Tehran, Iran

MS received 5 June 2015; accepted 24 June 2015

Abstract. **The aim of this study is to prepare core–shell $La_{0.73}Sr_{0.27}MnO_3$–silica nanoparticles and evaluating their heat generation ability under the safe alternating magnetic field ($f = 100$ kHz and $H = 10$–20 kA m^{-1}) for potential applications in magnetic fluid hyperthermia and magnetically triggered drug delivery systems. The magnetic cores of $La_{0.73}Sr_{0.27}MnO_3$ with an average particle size of 54 nm were synthesized by the citrate–gel method. Then, the Stober method was applied to encapsulate nanoparticles with 5-nm-thick silica shell. The core–shell structure of nanoparticles was confirmed by X-ray diffraction, fourier transform infrared spectroscopy and transmission electron microscopy analyses. Cytotoxicity of bare and silica-coated nanoparticles was evaluated by methyl thiazol tetrazolium bromide assay with MCF-7 cell line. The results revealed that the both samples have negligible toxicity below 500 μg ml^{-1} and silica coating can improve the biocompatibility of nanoparticle. In addition, calorimetric measurements were used to determine the heating efficiency of the core–shell nanostructures in aqueous medium. The results showed that the heat generated of the prepared sample could be safely controlled in the range of 40–60°C which is suitable for biomedical applications.**

Keywords. **Hyperthermia; core–shell; magnetic nanoparticles; biocompatibility; Stober method.**

1. Introduction

Nowadays, magnetic nanoparticles (MNPs), due to their particular physicochemical properties, have attracted growing interest in biomedicine and bioengineering such as magnetically triggered drug delivery,[1] bio-separation,[2,3] magnetic resonance imaging,[4] biomacromolecule purification[5] and magnetic hyperthermia.[6,7] Magnetic hyperthermia has long been used as a treatment option for cancer.[8] In this method MNPs are introduced to the tumour tissue and then exposed to an alternating magnetic field (AMF). This method leads to heat generation by the MNPs which can kill the cancerous cells.[6,7] In magnetically triggered drug delivery systems, MNPs are normally coated with a thermosensitive polymer as drug carrier. When these MNPs are exposed to an AMF, due to the heat generated by magnetic core, phase transition occurs in the thermosensitive polymer and drug releases.[9] The most common MNPs used for magnetic hyperthermia or drug delivery are Fe_3O_4 or γ-Fe_2O_3.[10–12] However, their use as heat generating agent is associated with a main drawback in related to the lack of *in vivo* control on the temperature of nanoparticles, which can cause local overheating and damage to surrounding healthy cells.

To overcome this problem, first option is monitoring temperature of tissue using an invasive thermometry to control the temperature by adjusting the AMF intensity. Another option is to take advantage of Curie temperature (T_c, temperature at which MNPs lose their magnetic properties) of MNPs as an intrinsic thermo-regulating property. Hence, the overheating can be hindered due to the change in the magnetic state of nanoparticles in the vicinity of the T_c.[13] Hence, by employing MNPs with T_c in the desired temperature range, the maximum attained temperature by MNPs can be controlled even with unwanted changes in magnetic field intensity. $La_{1-x}Sr_xMnO_3$ perovskite oxides with adjustable T_c in the body temperature range for $0.2 \leq x \leq 0.3$ are one of the particular interests for biomedical application.[14] Among the series of $La_{1-x}Sr_xMnO_3$ perovskite oxides the $La_{0.73}Sr_{0.27}MnO_3$ possesses highest saturation magnetization with T_c of about 70–80°C. Hence it is more suitable for biomedical application among all $La_{1-x}Sr_xMnO_3$ compounds. In order to prevent toxic effects of MNPs, the surface of nanoparticles is generally coated with an organic layer (polymer or surfactants) or inorganic layer (silica, carbon or precious metals) or combination of them.[15–19] Among various protective coatings, silica possesses several advantages as a coating shell for MNPs. The formation of silica shell on the surface of MNPs could hinder the magnetic dipolar attraction between particles, which improves their dispersibility and chemical stability in aqueous media and biological systems. Another advantage of silica coating is that the silanol or siloxane groups present on the surface of silica shell may be modified with various functional groups such as amines and carboxyl groups.[20–22]

*Author for correspondence (edrisi@aut.ac.ir)

In this research we focused on the preparation of MNPs based on $La_{0.73}Sr_{0.27}MnO_3$ (LSMO) as the self-controlled heating core and silica shell as protective layer which can be easily functionalized with targeting and drug releasing components. Cytotoxicity of bare and silica-coated nanoparticles was evaluated by MTT assay with MCF-7 cell line. Calorimetric measurements were then carried out to determine their ability for heat generation under the safe and harmless AFM ($H = 10$–20 kA m^{-1}, $f = 100$ kHz) used in our study.

2. Materials and methods

2.1 *Materials*

$La(NO_3)_3{\cdot}6H_2O$ (Sigma), $Sr(NO_3)_3$ (Merck), $Mn(NO_3)_2{\cdot}4H_2O$ (Merck), citric acid ($C_6H_8O_7$, Merck), ethylene glycol ($C_2H_6O_2$, Merck), tetraethylorthosilicate (TEOS), methanol, ethanol and ammonia solution (NH_4OH, 25 wt%, Merck) were all used as supplied without further purification.

2.2 *LSMO nanoparticles synthesis*

The citrate–gel method with optimized quantities was applied to synthesize the LSMO nanoparticles.[23–25] The metal nitrates were used as starting materials and weighed according to the stoichiometric composition of $La_{0.73}Sr_{0.27}MnO_3$ and dissolved in deionized water. The prepared solution was mixed with citric acid and ethylene glycol and then aqueous ammonia was added dropwise to adjust pH of solution to 9. The solution was then heated on a hot plate under constant stirring at 75–80°C to evaporate excess water and converting the solution to a viscous glassy gel. The gel was dried in an oven at 160°C and maintaining at this temperature overnight to produce dark greyish flakes. The flakes were ground and then calcined at 800°C for 4 h in box furnace with air atmosphere.

2.3 *Coating the LSMO nanoparticles with the silica shell*

Silica encapsulation process was performed according to the Stober method.[26] First, the surface of the LSMO nanoparticles (200 mg) was activated by sonication of nanoparticles in 1 M nitric acid solution at room temperature for 15 min. The nanoparticles were isolated by magnetic decantation using external magnet and redispersed in 0.1 M citric acid solution and sonicated for another 15 min. The nanoparticles were separated and washed with deionized water several times, and dispersed in water alkalized by adding some drops of ammonia solution.

The obtained solution was poured into a mixture of ethanol/water/ammonia with the final volume ratio of 70/28/2. To encapsulate the nanoparticles by silica shell, 1 ml TEOS was added to the reaction medium at 40°C with constant stirring. Finally, after 16 h, the obtained product was separated by centrifugation and washed with ethanol and water and dried at 50°C for 24 h.

2.4 *Characterization*

The X-ray diffraction (XRD) patterns of bare and silica-coated nanoparticles were obtained at room temperature by a Philips X'Pert powder diffractometer with CuKα radiation and Ni filter ($\lambda = 0.15418$ nm). Fourier transform infrared (FTIR) spectroscopy analysis was performed on a JASCO FTIR 680-Plus spectrometer in the region 400–4000 cm^{-1}. The morphology and particle size distribution of nanoparticles were examined using a Zeiss-EM10C transmission electron microscope (TEM) operated at an acceleration voltage of 80 kV. The magnetic properties of sample were obtained by a vibrating sample magnetometer (VSM) instrument.

2.5 *Cell viability study through the methyl thiazol tetrazolium bromide (MTT) assay*

In vitro cytotoxicity of the bare and silica-coated LSMO nanoparticles was evaluated using MTT assay. To this end, approximately 1×10^5 ml^{-1} cells (MCF-7) were seeded in a 96-well plate and incubated for 24 h at 37°C in a humidified 5% CO_2 atmosphere. The cells were treated with various concentrations (50, 100, 200, 400 and 500 µg ml^{-1}) of bare and polymer-coated nanoparticles and were cultured for another 24 h. After incubation, 15 µl of MTT reagent was added to each well and was further incubated for 4 h and then optical density was evaluated at 570 nm. Cell viability was calculated as follows:

$$\text{Cell viability}(\%) = [(A_{\text{sample}} - A_{\text{blank}})/(A_{\text{control}} - A_{\text{blank}})] \times 100\%, \quad (1)$$

where A_{sample} is the absorbance of a well containing cells, MTT solution, and bare or polymer-coated nanoparticles; A_{control} the absorbance of a well containing cells and MTT solution only; and A_{blank} the absorbance of a well containing medium and MTT solution only.

2.6 *Calorimetric measurements*

The heat generation ability of the silica-coated LSMO nanoparticles for biomedical application was investigated using a home-made induction heating instrument that induced an alternating magnetic field in five turns (5 cm diameter) induction coil. A close loop water temperature control was made to keep the temperature of the coil at ambient temperature. The stable suspension of silica-coated LSMO nanoparticles (50 mg ml^{-1}) in 1.5 ml plastic microtube, thermally insulated using styrofoam, was placed in the centre of coil and then irradiated by magnetic field ($f = 100$ kHz, $H = 10$–20 kA m^{-1}). The temperature of the sample was monitored by an alcohol thermometer. The value of the specific absorption rate (SAR) of the sample was calculated according to

$$\text{SAR} = \left(\frac{C_{\text{suspension}}}{X_{\text{NP}}}\right)\left(\frac{\mathrm{d}T}{\mathrm{d}t}\right), \quad (2)$$

where $C_{suspension}$ is the specific heat of the suspension ($C_{water} = 4.18$ J g^{-1} K^{-1} and $C_{NP} = 0.66$ J g K^{-1}),[27] X_{NP} is the weight fraction of nanoparticles ($X_{NP} = 0.05$) and dT/dt is the initial slope of the temperature curve *vs.* time.

3. Results and discussion

Silica-coated magnetic nanoparticles can be synthesized by various synthetic methods, among which the two most common methods are sol–gel process and microemulsion method.[26,28]

The sol–gel method, known as the Stober method, used mainly for the synthesis of silica nanoparticles, is also applied for the formation of silica shell on the surface of magnetic nanoparticles. As an alternative to the Stober method, the microemulsion method has been used for the preparation of silica-coated iron oxide nanoparticles.[29] Among these methods, the Stober method has been preferred more widely for synthesis of core–shell magnetic-silica nanoparticles, because of low cost, relatively mild reaction condition, and surfactant-free. Hence, in this research, the coating process of the LSMO nanoparticles was performed according to the Stober's method using TEOS in highly polar mixtures of ethanol, water and ammonia.

3.1 *XRD*

Figure 1a shows the crystalline structure of bare and silica-coated LSMO nanoparticles examined by XRD analysis. In XRD pattern of bare nanoparticles, all reflection peaks can be well indexed with Joint Committee on Powder Diffraction Standards (JCPDS) (Card no.: 00-051-0409) and correspond to cubic perovskite structure (space group R-3C).[30] No peak of any secondary or impurity phase is observed in the XRD pattern of bare nanoparticles, indicating the high purity of sample. When the LSMO nanoparticles were coated with silica, a broad band near $2\theta \sim 24°$ was detected, indicating the existence of amorphous SiO_2 shell on the surface of nanoparticles.[31] Also, the position of all reflection peaks on both XRD patterns remains similar, which demonstrates that the crystal structure of LSMO nanoparticles embedded in silica shell does not change after the coating process. Also, the average crystallite size (D_{XRD}) of LSMO nanoparticles was determined using Scherrer's equation:

$$D = 0.9\lambda/\beta\cos\theta, \tag{3}$$

where λ is the incident X-ray wavelength ($\lambda_{Cu} = 1.5443$ Å), β and θ the full-width at half-maximum (FWHM) and diffraction angle of the peak corresponding to maximum intensity, respectively. The average crystallite size of bare nanoparticles was calculated by applying equation (3) to the major reflection peak of XRD spectrum at $2\theta = 32.73°$ and was about 48.8 nm.

3.2 *FTIR analysis*

The crystalline structure of the LSMO perovskite oxides is similar to the distorted $GdFeO_3$-type structure in which a central Mn cation is octahedrally surrounded by six oxygen onions. The MnO_6 has nearly ideal octahedral symmetry with six vibrational modes, but only two of them are activated using IR irradiation.[32] The band around 600 cm^{-1} is related to the stretching mode (ν_s) of Mn–O or Mn–O–Mn bonds, and the band around 400 cm^{-1} corresponds to the bending mode (ν_b) of Mn–O–Mn bond, which is due to the change in the bond angle.[33] The FTIR spectra of bare and coated LSMO nanoparticles are shown in figure 1b. In FTIR spectrum of uncoated nanoparticles, the absorption bands around 595 and 400 cm^{-1} can be observed, which are related to the stretching mode and bending mode of Mn–O–Mn, respectively. The appearance of these bands suggests that the LSMO nanoparticles with perovskite structure have been formed at 800°C, which is in agreement with XRD result.

In order to confirm the presence of the silica shell on the surface of LSMO nanoparticles, after coating process, FTIR analysis was performed on the obtained sample and the result is shown in figure 1b. Compared to the uncoated LSMO nanoparticles, some new absorption peaks have appeared in FTIR spectrum. The peaks at 468.3, 801.4 and 1085.5 cm^{-1}

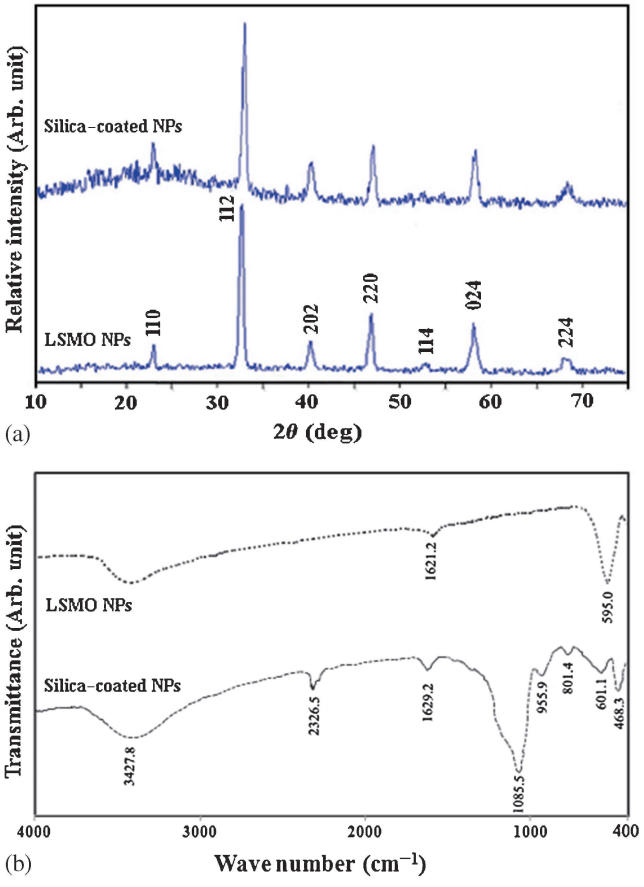

Figure 1. (**a**) XRD patterns and (**b**) FTIR spectra of bare and silica-coated LSMO nanoparticles.

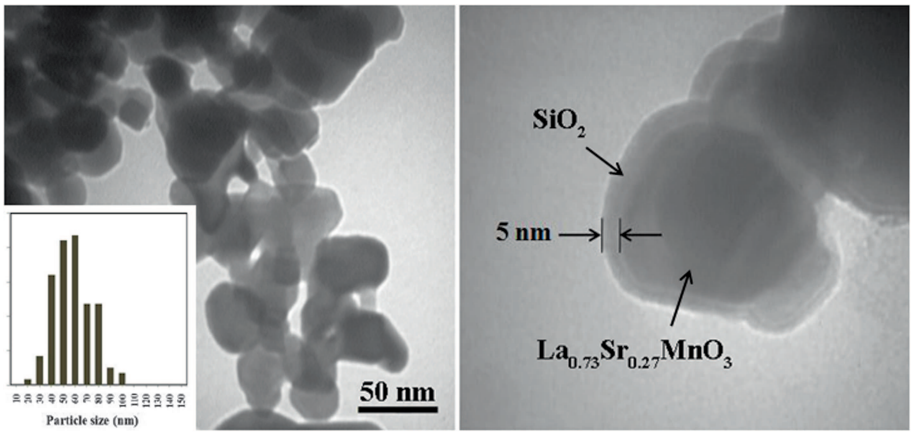

Figure 2. TEM images of (**a**) bare LSMO nanoparticles (inset shows particle size distribution) and (**b**) core–shell structure of silica-coated nanoparticles.

are assigned to the bending vibration, symmetric, and asymmetric stretching vibration of Si–O–Si bond, respectively. The appeared band at 955.9 cm^{-1} corresponds to the bending vibration of Si–OH. The absorption bands at around 1620 and 3427 cm^{-1} in two spectra are due to the stretching and bending modes of H–O–H, free or adsorbed on the surface of nanoparticles, respectively. The characteristic absorption bands of LSMO nanoparticles also have appeared at 601.1 cm^{-1} in the spectrum of silica-coated LSMO nanoparticles but with smaller intensity. This can be explained by the fact that the surface of the nanoparticles is coated by thin SiO_2 shell.

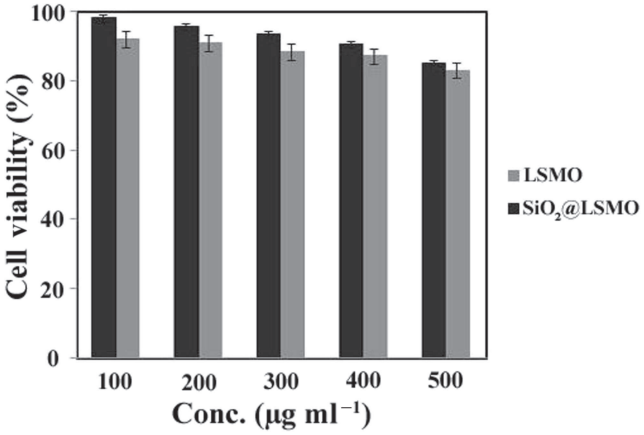

Figure 3. Cytotoxicity of bare and silica-coated LSMO nanoparticles at different concentrations.

3.3 *TEM analysis*

Figure 2a shows TEM image of nanocrystalline LSMO synthesized at 800°C. The inset of figure 2a shows the corresponding particle size distribution histogram of sample, which is calculated based on the Feret-diameter for more than 200 particles from several images. The average particles size distribution (D_{TEM}) is about 54 nm which is larger than the result obtained by Scherrer's equation, due to the attachment of crystalline primary particles during calcination process.[34] Similar results have also been reported previously.[35]

The effect of particle size on the durability of MNPs *in vivo* has been investigated by several researchers.[36,37] It has been found that particles with sizes in the range of 10–100 nm are optimal for long circulation times *in vivo*. Nanoparticles large than 200 nm are easily isolated by the macrophage cells or phacocytic cells in the spleen.[36] Ultrasmall MNPs (<10 nm) are rapidly removed by the renal system.[37] Hence, the nanoparticles obtained in this study with 54 nm average particle size are suitable for biomedical applications. The TEM image of silica-coated LSMO nanoparticles is shown in figure 2b. In this figure, the formation of core–shell structure can be confirmed by two distinguishable regions with different electron densities. A high electron density (darker) region is related to magnetic core and a transparent (low electron density) region surrounding core corresponds to the silica shell with thickness of about 5 nm.

3.4 *Biocompatibility study*

The MTT assay was used to estimate the cytotoxicity of synthesized samples. Figure 3 shows the cell viability of MCF-7 cells after 24 h exposure to the bare and silica coated nanoparticles at different concentrations (100, 200, 300, 400 and 500 μg ml^{-1}). It can be clearly observed that the percent of cell viability depends on the concentration of nanoparticles in the cell culture media and decreased upon increasing nanoparticles concentration. Also, for the same concentration of samples, the polymer-coated nanoparticles is more biocompatible than the bare particles. For all concentrations, the values of the cell toxicity are less than 17%. These results

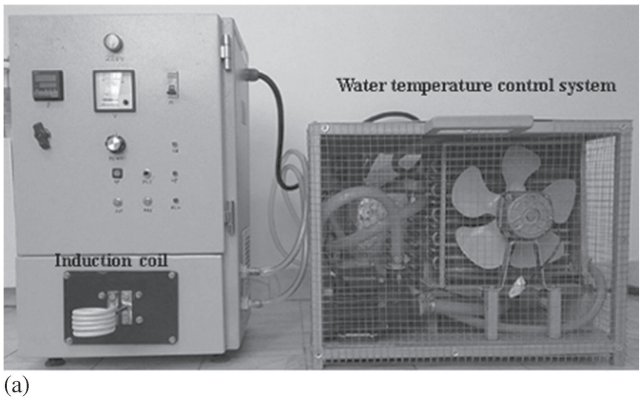

(a)

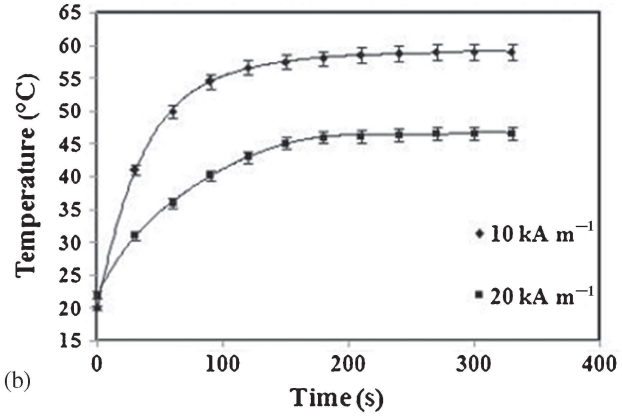

(b)

Figure 4. (**a**) Induction heating unit used for calorimetric measurement and (**b**) temperature *vs*. time for aqueous suspension of silica-coated LSMO nanoparticles at different magnetic fields.

indicate that the both prepared samples exhibit low cytotoxicity, satisfying one of the major requirements for biomedical applications.

3.5 *Magnetic properties*

Saturation magnetization (M_s) and the Curie temperature of bare LSMO nanoparticles, measured by the VSM method, were 39 emu g^{-1} and 344 K (75°C), respectively. It should be remarked that this temperature corresponds to the complete demagnetization of sample and the maximum temperature achievable by nanoparticles exposed to a finite and specific magnetic field used in biomedical application should be determined by calorimetric measurements. The induction heating instrument used for calorimetric measurement is shown in figure 4a. The temperature *vs*. heating time for aqueous suspension of silica-coated nanoparticles (50 mg ml^{-1}) exposed to the alternating magnetic field with different intensities ($H = 10$ and 20 kA m^{-1}, $f = 100$ kHz) are shown in figure 4b. As can be observed from figure 4b, after a short time (less than 3 min), the temperature of suspension is saturated at $T_{max} = 46$ and 59°C for $H = 10$ and 20 kA m^{-1}, respectively. This saturation is due to the decreasing of the magnetization near the T_c and the balance of heat exchange with surrounding medium. Also, the heating curves show that the maximum temperature of magnetic suspension falls within the desired temperature range (40–60°C) which suggests that the prepared samples are suitable for biomedical applications. In addition, the SAR values of samples were 47.3 and 77.8 W g_{NPs}^{-1} for magnetic intensities of 10 and 20 kA m^{-1}, respectively.

4. Conclusions

Magnetic LSMO nanoparticles were successfully synthesized by the citrate–gel method. This synthesis technique resulted in nanoparticles with an average particle size of 54 nm. The pure obtained nanoparticles were then successfully encapsulated with 5-nm-thick silica shell, employing a procedure derived from the Stober method. The formation of silica shell on the surface of nanoparticles was confirmed by XRD, FTIR and TEM analyses. Cytotoxicity of bare and silica-coated nanoparticles was evaluated by MTT assay with MCF-7 cell line. The results revealed that the both samples have negligible toxicity below 500 μg ml^{-1}. Heating experiments at safe magnetic field ($f = 100$ kHz, $H = 10$–20 kA m^{-1}) revealed that the maximum achieved temperature of water stable silica-encapsulated nanoparticles (50 mg ml^{-1}) are fully in agreement with biomedical applications.

References

1. Mc Bain S C, Yiu H H and Dobson J 2008 *Int. J. Nanomed.* **3** 169
2. Tibbe A G J, de Grooth B, Greve J, Liberti P A, Dolan G J and Terstappen L W M M 1999 *Nat. Biotechnol.* **17** 1210
3. Liberti P A, Rao C G and Terstappen L W M M 2001 *J. Magn. Magn. Mater.* **225** 301
4. Zhang M, Jugold E, Woenne T, Lammers B, Morgenstern M M, Mueller H, Zentgraf M, Bock M, Eisenhut M, Semmler W and Kiessling F 2007 *Cancer Res.* **67** 1555
5. Elaissari A, Rodrigue M, Meunier F and Herve C 2001 *J. Magn. Magn. Mater.* **225** 127
6. Jordan A, Scholz R, Wust P, Fahling H and Felix R 1999 *J. Magn. Magn. Mater.* **201** 413
7. Jordan A, Scholz R, Wust P, Schirra H, Schiestel T, Schmidt H and Felix R 1999 *J. Magn. Magn. Mater.* **194** 185
8. Soares P I, Ferreira I M, Igreja R A, Novo C M and Borges J P 2012 *Rec. Patent Anticancer Drug Discov.* **7** 64
9. Purushotham S, Chang P E J, Rumpel H, Kee I H C, Ng R T H, Chow P K H, Tan C K and Ramanujan R V 2009 *Nanotechnol.* **20** 305101
10. Linh P H, Thach P V, Tuan N A, Thuan N C, Manh D H, Phuc N X and Hong L V 2009 *J. Phys.: Conf. Ser.* **187** 012069
11. Majeed J, Pradhan L, Ningthoujam R S, Vatsa R K, Bahadur D and Tyagi A K 2014 *Colloid Surf. B* **122** 396
12. Yu J H, Lee J S, Choa Y H and Hofmann H J 2010 *Mater. Sci. Technol.* **26** 333
13. Kuznetsov A A, Shlyakhtin O A, Brusentsov N A and Kuznetsov O A 2002 *Eur. Cell. Mater.* **3** 75

14. Asamitsu A, Morimoto Y, Kumai R, Tomioka Y and Tokura Y 1996 *Phys. Rev. B* **54** 1716
15. Lu A H, Salabas E L and Schuth F 2007 *Angew. Chem. Int. Ed.* **46** 1222
16. Sun C, Lee J S H and Zhang M 2008 *Adv. Drug Deliv. Rev.* **60** 1252
17. Nasongkla N, Bey E, Ren J, Ai H, Khemtong C, Guthi J S, Chin S F, Sherry A D, Boothman D A and Gao J 2006 *Nano Lett.* **6** 2427
18. Jeong U, Teng X, Wang Y, Yang H and Xia Y 2007 *Adv. Mater.* **19** 33
19. Laurent S, Forge D, Port M, Roch A, Robic C, Elst L V and Muller R N 2008 *Chem. Rev.* **108** 2064
20. Philipse A P, van Bruggen M P B and Pathmamanoharan C 1994 *Langmuir* **10** 92
21. Liu Q, Xu Z, Finch J A and Egerton R 1998 *Chem. Mater.* **10** 3936
22. Liu X Q, Ma Z Y, Xing J M and Liu H Z 2004 *J. Magn. Magn. Mater.* **270** 1
23. Soleymani M, Moheb A and Joudaki E 2009 *Cent. Eur. J. Chem.* **7** 809
24. Edrissi M, Soleymani M and Akbari S 2011 *Synth. React. Inorg. M.* **41** 1282
25. Edrissi M, Hosseini S A and Soleymani M 2011 *Micro. Nano Lett.* **6** 836
26. Edrissi M, Soleymani M and Adinehnia M 2011 *Chem. Eng. Technol.* **34** 1813
27. Kim D, Zink B L, Hellman F and Coey J M D 1994 *Phys. Rev. B* **65** 214424
28. Tago T, Harsuta T, Miyajima K, Kishida M, Tashiro S and Wakabayashi K 2002 *J. Am. Ceram. Soc.* **85** 2188
29. Narita A, Naka K and Chujo Y 2009 *Colloids Surf. A* **336** 46
30. Sayagues M J, Cordoba J M and Gotor F J 2012 *J. Solid State Chem.* **188** 11
31. Singh R K, Kim T H, Patel K D, Knowles J C and Kim H W 2012 *J. Biomed. Mater. Res. A* **100A** 1734
32. Liu Sh, Tan X, Li K and Hughes R 2002 *Ceram. Int.* **28** 327
33. Wang X, Cui Q, Pan Y and Zou G 2003 *J. Alloys Compd.* **354** 91
34. Naravanaswamy A, Xu H F, Pradhan N and Peng X G 2006 *Angew. Chem. Int. Ed.* **45** 5361
35. Lopez-Quintela M A, Hueso L E, Rivas J and Rivadulla F 2003 *Nanotechnol.* **14** 212
36. Tabata Y and Ikada Y 1990 *Adv. Polym. Sci.* **94** 107
37. Choi H S, Liu W, Misra P, Tanaka E, Zimmer J P, Ipe B I, Bawendi M G and Frangioni J V 2007 *Nat. Biotechnol.* **25** 1165